APPLIED AND ENVIRONMENTAL MICROBIOLOGY, Sept. 1995, p. 3329–3335 Vol. 61, No. 9
0099-2240/95/$04.00+0

Determination of Effective Transport Coefficients for Bacterial Migration in Sand Columns

JOHN W. BARTON† AND ROSEANNE M. FORD*

Department of Chemical Engineering, University of Virginia, Charlottesville, Virginia 22903

Received 28 February 1995/Accepted 10 July 1995

A well-characterized experimental system was designed to evaluate the effect of porous media on macroscopic transport coefficients which are used to characterize the migration of bacterial populations. Bacterial density profiles of *Pseudomonas putida* PRS2000 were determined in the presence and absence of a chemical attractant (3-chlorobenzoate) gradient within sand columns having a narrow distribution of particle diameters. These experimental profiles were compared with theoretical predictions to evaluate the macroscopic transport coefficients. The effective random motility coefficient, used to quantify migration due to a random process in a porous medium, decreased nearly 20-fold as grain size in the columns decreased from 800 to 80 μm. The effective random motility coefficient μ_{eff} was related to the random motility coefficient μ, measured in a bulk aqueous system, according to $\mu_{eff} = (\varepsilon/\tau)\mu$ with porosity ε and tortuosity τ. Over the times and distances examined in these experiments, bacterial density profiles were unaffected by the presence of an attractant gradient. Theoretical profiles with the aqueous phase value of the chemotactic sensitivity coefficient (used to quantify migration due to a directed process) were consistent with this result and suggested that any chemotactic effect on bacterial migration was below the detection limits of our assay.

Motile bacteria capable of sensing chemical gradients within their environment are attracted to amino acids, sugars, and other substances that are beneficial to them; they are similarly repelled by harmful substances, such as acetate, and extremes of pH (17, 19–21). This phenomenon, known as chemotaxis, is believed to play an important role in the ability of subsurface microbial populations to locate and move toward food sources (14, 18). It has been suggested (14, 18, 27) that chemotaxis may be one mechanism that can be exploited for increasing the overall effectiveness of biodegradation as a treatment process by facilitating contact between bacteria and the contaminant to be degraded. To evaluate the role of bacterial migration in such a process, it is necessary to quantitatively describe the migration behavior of bacterial populations in both the presence and absence of chemical gradients within natural systems involving porous media.

Certain *Pseudomonas putida* strains are known to be chemotactic toward a variety of aromatic acids, including benzoate and 3-chlorobenzoate (3CB), and a benzoate chemoreceptor has been identified (11, 13). Our studies have focused on *P. putida* PRS2000, which like many pseudomonad strains, possesses multiple polar flagella. Typically there are five to seven flagella located at one end, each 5 to 10 μm in length (12). When the flagella rotate together in a counterclockwise direction, cells swim roughly in a straight line at an average cell swimming speed of 44 μm/s. These runs typically last from 1 to 3 s and are separated by a brief (30 to 50 ms) reversal in the direction of flagellar rotation. During this reversal, the bacterial body is reoriented so that a new direction or path is undertaken. This change of direction is mechanically different from that exhibited by *Escherichia coli* cells, which have peritrichous flagella that cause the cell to tumble when flagellar rotation is reversed. However, except for a few details which can be attributed mainly to differences in flagellar arrangement, the motile behavior of *P. putida* appears to be very similar to that of *E. coli* (12). In the absence of chemical gradients, this behavior (known as random motility) results in a random walk analogous to molecular diffusion. When an attractant gradient is imposed upon chemotactic bacteria, cells bias their motion by increasing their smooth-swimming run times (or decreasing the frequency at which they change direction) when moving toward increasing concentrations. A significant research effort has been conducted to characterize such behavior for cell populations in terms of the individual bacterial properties which govern the behavior just described (5–9). Within a porous medium characterized by pore diameters smaller than the average run length of bacteria in the bulk, individual bacterial trajectories may be altered because of collisions with the matrix, thus impacting the rate at which the population spreads through the porous medium.

Our approach extends model equations developed by Rivero et al. (23) for bulk aqueous systems to characterize bacterial density profiles in stagnant aerobic porous systems for *P. putida*. Fundamental transport coefficients, the random motility and chemotactic sensitivity coefficients defined by Rivero et al., are replaced in the model equations by effective values for our application to porous media. Experimental results are compared with a theoretical expression by Duffy et al. (4) for the effective random motility coefficient which depends on properties of the porous media such as grain size.

MATERIALS AND METHODS

Bacterial strains and growth conditions. *P. putida* PRS2000 cells were obtained on agar slants from Wayne Coco at the University of Illinois at Chicago. Frozen stocks were made by addition of 0.5 ml of 40% glycerol to 0.5 ml of an overnight culture grown in a mineral medium solution containing 5 mM sodium benzoate as a carbon source and were stored at −70°C. For experiments, a loopful (inoculating loop) of cells was scraped from frozen stock and inoculated into a well-defined mineral base as used in the laboratory of D. T. Gibson at the University of Iowa (10). The formulation was a variation of one published earlier

* Corresponding author. Phone: (804) 924-6283. Fax: (804) 982-2658. Electronic mail address (Internet): rmf3f@virginia.edu.

† Present address: Chemical Technology Division, Oak Ridge National Laboratory, Oak Ridge, TN 37831.

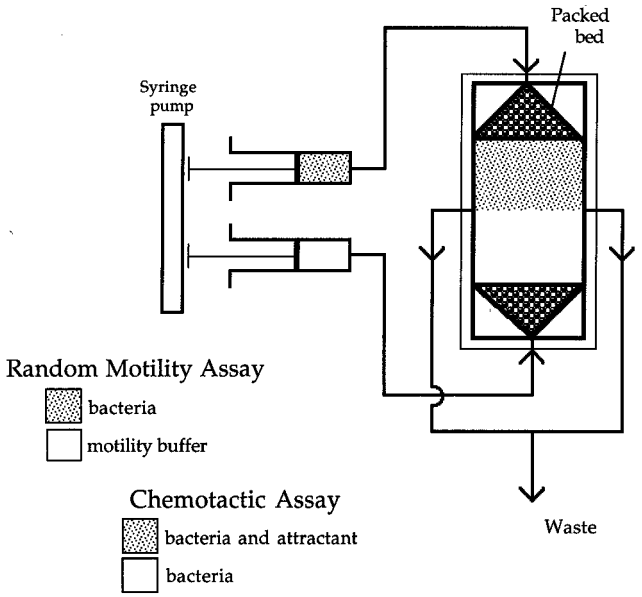

FIG. 1. Schematic representation of the SFDC assay. The chamber is a sealed system formed by two microscope slides which are separated by a 0.19-cm gap. Fluid enters the top and bottom ports and exits the chamber through side ports at the midpoint. Triangular beds of nylon beads disperse momentum associated with incoming fluid and evenly distribute flow across the chamber's width.

by Cohen-Bazire et al. (3). It was prepared by dilution of three stock solutions: A, a buffer portion; B, mineral base; and C, a solution of ammonium sulfate. Solution A contained 141.2 g of Na_2HPO_4 and 136 g of KH_2PO_4 per liter of distilled water. Solution B contained 10 g of nitriloacetic acid, 14.45 g of $MgSO_4$, 3.33 g of $CaCl_2 \cdot 2H_2O$, 9.25 mg of $(NH_4)_6Mo_7O_{24} \cdot 4H_2O$, 99 mg of $FeSO_4 \cdot 7H_2O$, and 50 ml of Metals 44 solution (3) per liter of distilled water. Solution C contained 200 g of $(NH_4)_2SO_4$ per liter of distilled water. To prepare 1 liter of the medium, 40 ml of solution A, 20 ml of solution B, and 5 ml of solution C were diluted to 1 liter with distilled water. A carbon source (filter sterilized) was added after autoclaving. The pH of the medium was 6.8. Cultures were incubated at 30°C and aerated by shaking at 150 rpm (in a LabLine Orbital shaker, model 3520) for periods of 20 to 30 h to stationary-phase cell densities of approximately 5×10^8 cells per ml. Cells were observed under a phase-contrast microscope at ×400 to qualitatively check for motility and contamination. Approximately 95 to 100% of the cells were motile in the cultures used for experiments. For both random motility and chemotaxis stopped-flow diffusion chamber (SFDC) assays, 2.0 ml of this suspension was diluted 50-fold in motility buffer (11.2 g of K_2HPO_4, 4.8 g of KH_2PO_4, and 0.029 g of EDTA per liter of distilled water), which had a pH of 7.0.

3CB was used as the chemical attractant for *P. putida* at concentrations of 5.0 mM. 3CB, a structural analog of benzoate, uses the same receptor system as benzoate and elicits a chemotactic response but cannot be metabolized (15); use of 3CB as an attractant eliminates complications that might arise because of uptake, such as secondary metabolite gradients. Benzoate was used as a carbon source during growth and is necessary for inducing the production of benzoate-binding receptors (proteins of the chemosensory system necessary for a chemotactic response) (15).

SFDC assay. The SFDC assay, developed by Ford et al. (6, 7), provided a well-characterized and reproducible method for measuring bacterial transport coefficients in aqueous media (Fig. 1). Within the chamber, two suspensions differing in attractant and/or cell concentration were contacted by impinging flow. As long as fluid was flowing, the upper suspension did not mix with the lower one, which created well-defined initial conditions within the chamber. In both random motility and chemotaxis assays, redistribution of the bacterial population was recorded over a 10-min period after flow had been stopped by capturing digitized microscopic images of scattered light (Zeiss STEMI SV8 microscope, Dage MTI CCD72 video camera, Mass Microsystems' Quickimage 24). Subsequent analysis of these images (with NIH Image 1.44 for Macintosh OS) provided a representation of bacterial density profiles, which were used to determine the transport coefficients, μ_0 and χ_0.

For random motility studies, diluted bacterial suspension was introduced into the upper half of the chamber only. No attractant was added to either half. During flow, a sharp interface was observed between the upper and lower halves of the chamber. Once flow was stopped, bacteria in the upper half of the chamber began swimming across the midpoint, and the interface became less distinct as time progressed. On the basis of Stokes' law calculations, cell settling velocities (due to gravity) are low compared with the average swimming speed; gravitational effects on cell migration are thus negligible (7).

For chemotaxis assays, fluid introduced into the upper half of the chamber contained only dilute bacterial suspension ($\sim 1 \times 10^7$ cells/ml). In the bottom half, dilute bacterial suspension contained appropriate amounts of attractant (5 mM 3CB). Initially, while the solutions were flowing through the chamber, bacterial density was uniform, and a step change in attractant concentration was maintained at the midpoint. When flow was stopped, attractant in the bottom half of the chamber began to diffuse into the upper half, forming a concentration gradient. Chemotactic bacteria sensed and responded to this gradient, causing a band of high cell density to form immediately and to move downward toward higher attractant concentrations as time progressed. Above the concentrated band lay a darker band of low cell density. Both bands broadened with time.

Conservation equations for the attractant concentration, a, and the bacterial density, b, in one spatial dimension, x, were

$$\frac{\partial a}{\partial t} = -\frac{\partial (J_a)}{\partial x} \tag{1}$$

$$\frac{\partial b}{\partial t} = -\frac{\partial (J_b)}{\partial x} \tag{2}$$

with attractant and bacterial fluxes, J_a and J_b, respectively. In their original phenomenological model, Keller and Segel (16) proposed an expression for bacterial flux

$$J_b = -\mu \frac{\partial b}{\partial x} + V_c b \tag{3}$$

which included one term to describe diffusion-like or random motility behavior and a second term for convection-like or chemotactic motion. The random motility coefficient, μ, was analogous to a molecular diffusion coefficient, and V_c was the chemotactic velocity. The driving force for the chemotactic response was the attractant gradient, and therefore V_c was a function of the attractant gradient. The specific dependence

$$V_c(a) = s \tanh\left\{\frac{\chi_0}{s} \frac{K_d}{(K_d + a)^2} \frac{\partial a}{\partial x}\right\} \tag{4}$$

was derived previously by Rivero et al. (23), where s is the average one-dimensional cell swimming speed (equivalent to $v/2$, where v is the experimentally observed swimming speed [5]), χ_0 is the chemotactic sensitivity coefficient, and K_d is the dissociation constant. Rivero et al. (23) showed that in general, the random motility coefficient is also a function of the attractant gradient. However, for the experimental systems to which we applied this equation, the attractant gradient had a negligible effect on the random motility coefficient, and in our analysis we were able to replace μ in equation 3 with its gradient-independent value, μ_0.

Fick's first law (2) was used to describe the attractant flux

$$J_a = -D \frac{\partial a}{\partial x} \tag{5}$$

with the attractant diffusion coefficient, D. Except in simplifying cases, these coupled equations were solved numerically with a FORTRAN program incorporating a finite element IMSL subroutine for the boundary (no-flux) and initial conditions described in the experimental procedure.

Theoretical predictions were compared with digitized images of experimental profiles to obtain both the random motility and chemotactic sensitivity coefficients. Details of this analysis have been reported previously (6, 7, 9). For application to porous media, we replaced the transport coefficients μ and χ_0 in equations 3 and 4 with their effective values μ_{eff} and $\chi_{0,eff}$, which account for the impact of the porous media.

Sorption experiments. Batch studies were used to test for adsorption of bacteria and chemoattractant to silica sand. A bacterial solution of known concentration (6.3×10^8 cells per ml) was added to 15.0 g of dry, sterile sand until the sand was saturated. This solution was prepared by centrifugation (Jovan model CR 4.11) of a batch-grown solution for 10 min at 3,500 rpm and then resuspension of the pellet in mineral medium containing no available substrate. Nine batch flasks were prepared in this manner. Three flasks were immediately analyzed for aqueous-phase cell density. At 1 and 24 h, three more flasks were analyzed for aqueous-phase cell densities. Densities were determined by cultural counts as described previously, with three replicate plates for each dilution level.

Similar experiments were conducted to determine if significant amounts of the chemoattractant were adsorbed by silica sand. Five flasks each for 3CB were prepared as follows. Zero, 1, 5, 10, and 30 g of silica sand were added to 10 ml of mineral medium containing 5 mM attractant. The last flask (30 g) was only partially saturated. Each flask was shaken vigorously several times during the following 24 h to promote equilibrium conditions. After 24 h, each flask was

analyzed for aqueous-phase concentrations of attractant by high-performance liquid chromatography (HPLC).

Column experiments. Commercially available granular crystalline silica sand (Unimin Corp.) was sieved to obtain narrow particle size distributions for average diameters ranging from 80 to 800 μm. Sieving was conducted for 12 to 24 h in stainless steel sieve trays for sample sizes of 500 g of sand. Once separated, sand was then treated with 1.0 N H_2SO_4 for 1 h to remove organic matter that might serve as a carbon source or promote bacterial adsorption. Sand was then rinsed with tap water until the pH reached that of the tap water. Distilled water was used for three final rinses to remove many of the dissolved ions present in the tap water. Sterilization and drying occurred simultaneously in an oven at a temperature of 130°C over a 3-day period. Plate counts of sand samples after sterilization indicated that no viable microbes remained.

Sterile, graduated polypropylene tubes (FisherBrand) with an internal diameter of 2.5 cm were used for column experiments. For studies of random motility, a bacterial suspension initially saturated the bottom half of the column, while sterile mineral media saturated the upper half. As time progressed, bacteria would migrate upward. After a given incubation period, typically 24 h, columns were sectioned and each section was analyzed for viable cells. Sections, depending on the location within the column, were 2.5 or 5.0 mm in depth. The length of column containing saturated silica sand was 6 cm. For chemotaxis experiments, bacteria were initially placed only in the bottom of the column, while sterile mineral medium containing 5 mM 3CB saturated the top. Migration and diffusion were then allowed to take place for a 24-h period before the columns were sectioned and analyzed for both bacterial density and attractant concentration profiles.

Layering of columns to create step gradients was achieved by first adding dry sand, followed by the aqueous phase with a micropipette (Eppendorf). Layers were added sequentially in this manner in 2.5-mm increments. For example, in columns for random motility studies, dry sand was added to a depth of 2.5 mm and then saturated with a bacterial suspension. This step was repeated 12 times to give a total of 3 cm of saturated sand with a uniform bacterial density in the bottom half of the column. The remaining 3 cm of the column was prepared in a similar manner by using a mineral medium instead of a bacterial suspension to saturate the increments of dry sand. For chemotaxis studies, a bacterial suspension was used to saturate the 12 increments in the bottom 3 cm of the column and mineral medium with a 3CB concentration of 5 mM was used to saturate the 12 increments in the top 3 cm of the column. For the diffusion experiment with 3CB, mineral medium was used to saturate the 16 increments in the bottom 4 cm of the column and mineral medium augmented with 5 mM 3CB was used to saturate the 8 increments in the top 2 cm of the column. Dye studies showed that this method yielded sharp, reproducible step gradients and minimized convection. Another packing method was also investigated; wet packing the layers (adding previously saturated sand to columns) yielded sharp interfaces but tended to result in significant air entrainment. Vertically mounted columns were sectioned by removing layers from the top downward. A known volume (~3 ml) of sterile mineral medium was added to each layer removed. Samples were placed in an ice bath until they could be analyzed (from 0 to 12 h).

For analysis, each sample was vortexed for 30 s (Thermolyne Maxi Mix II). A sample of the supernatant was then filtered (Gelman 0.22-μm-pore-diameter Acrodiscs) to remove bacteria and sand prior to HPLC analysis (Waters HPLC system, Whatman C8 reverse-phase Partisphere column). Dilution series of the supernatant were also prepared for direct counts on nutrient agar (Difco). Two replicates were counted for each dilution level.

RESULTS

SFDC assay. The SFDC assay developed by Ford et al. (7) was utilized to determine the random motility and chemotactic sensitivity coefficients for *P. putida* PRS2000 in bulk aqueous media ($\varepsilon = 1$). The maximum value (without decay) measured for the random motility coefficient of *P. putida* PRS2000 was $(3.5 \pm 2.0) \times 10^{-5}$ cm^2/s. *P. putida* PRS2000 was found to have a chemotactic sensitivity coefficient of $(1.9 \pm 0.7) \times 10^{-4}$ cm^2/s in response to 5 mM 3CB. Approximately 20 h after inoculation, *P. putida* entered the stationary phase of growth. During this phase, the motility of the population decreased exponentially with time, presumably because of nutrient or oxygen deprivation (Fig. 2). After about 70 h, motility was reduced to the extent that it could not be measured accurately with the SFDC assay. This study was conducted because column experiments typically involve incubation periods of 24 h, during which changes in motility must be quantified to properly characterize the system. The specific decay rate, k_{decay}, for the random motility coefficient measured in the SFDC assay was found to be 0.14/h. We assumed this same rate coefficient would apply in the porous medium column studies. Thus, the equation

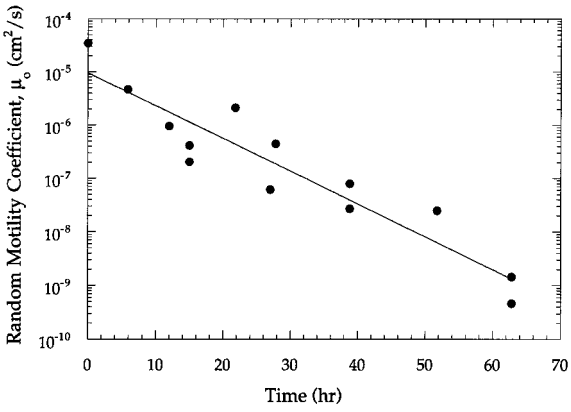

FIG. 2. Time-dependent decrease in bacterial random motility coefficient. In the absence of additional substrate added during the stationary phase of batch growth, motility decreases with time. The solid line represents an exponential fit of experimental points ($R = 0.945$), yielding a specific decay rate of 0.14/h.

$$\mu_{eff} = \mu_{0,eff}^{\max} exp(-k_{decay}t) \quad (6)$$

was coupled with the model equations to determine the maximum effective random motility coefficient in the absence of chemical gradients $\mu_{0,eff}^{\max}$.

Sorption to sand. In batch adsorption experiments over the course of 24 h, measured cell density in the aqueous phase deviated less than 5%, with no apparent decreasing trend with time. These small deviations were within the expected experimental error associated with the plate-counting technique for cultural counts.

Microscopic observations of Gram-stained bacteria on silica particles supported these results, revealing that only a few bacteria were captured by sand surfaces, primarily in crevices or cracks. Assuming that no more than 10 bacteria were captured per particle, we have estimated the number of bacteria captured on the surface to be negligible compared with the total aqueous-phase density.

Results from the sorption experiments with the chemoattractant also indicated that sorption to the sand was negligible. All values deviated from the initial concentrations used by less than 8%, and no decreasing trends were evident.

Verification of sampling procedure. Initial measurements of attractant diffusion coefficients were conducted in sterile sand columns to test experimental techniques and sampling procedures. In these experiments, a step gradient in 3CB was created within a column and allowed to incubate for 24 h. With the aqueous-phase diffusion coefficient of 3CB (calculated with the Wilke-Cheng relationship from the known value for benzoate [1]), a comparison of experimental data with theoretical predictions was possible and is represented in Fig. 3 for 3CB diffusion. Good correlation was achieved with a profile generated from the solution of equations 1 and 5 with a diffusion coefficient modified to account for porosity, confirming earlier visual experiments with dyes to check the reliability of the method. No-flux boundary conditions were used for the theoretical solution.

Bacterial density profiles at various times. In order to select an appropriate time over which to incubate columns, seven columns were constructed with *P. putida* PRS2000 suspension saturating the bottom half of the column and sterile mineral

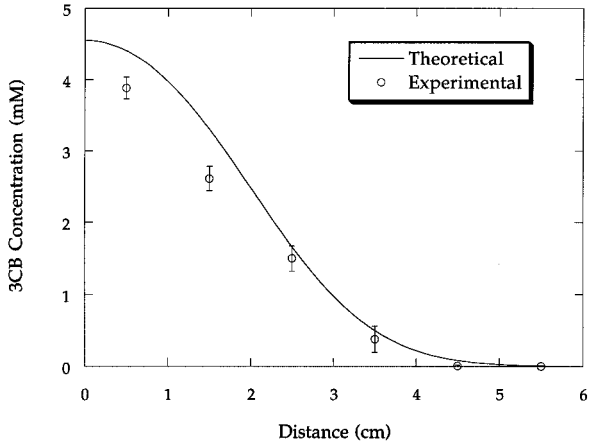

FIG. 3. Diffusion of 3CB within sand columns. Initially, 5 mM 3CB was placed in the tops of columns from 0 to 2 cm in depth. No bacteria were present, and the columns were allowed to stand for 24 h. Each point represents an average of four points from four replicate column experiments. The diffusion coefficient for 3CB used to generate the theoretical curve was 1.21×10^{-5} cm^2/s. The porosity was 0.37. No-flux boundary conditions exist at the top and bottom of the column.

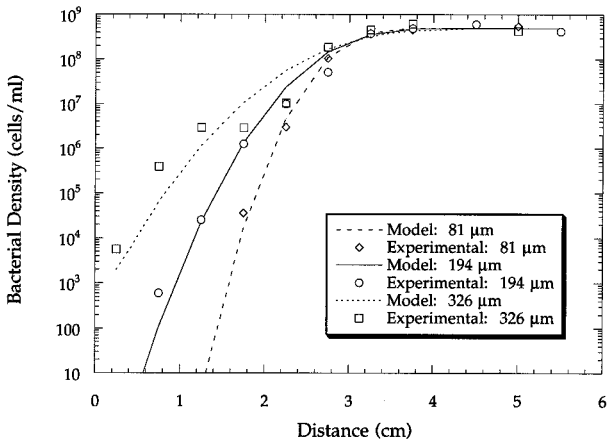

FIG. 5. Effect of grain size on bacterial density profiles in sand columns. Three sets of experimental points corresponding to three different particle diameters are shown. Lines drawn through points represent model predictions. Values of the effective random motility coefficients obtained for particle diameters of 81, 194, and 326 μm were 0.7×10^{-6}, 1.6×10^{-6}, and 3.1×10^{-6} cm^2/s, respectively.

medium saturating the top half. These columns were allowed to stand undisturbed for various lengths of time. One column was sectioned immediately; two columns were sectioned at 12, 24, and 96 h after construction. Sections were then analyzed for bacterial density (Fig. 4). As expected, sharper profiles were obtained at earlier incubation times. For subsequent experiments, we chose 24 h as a standard incubation time during which significant microbial population penetration would occur. The average particle diameter for silica sand used in this experiment was 200 μm. Sand had not been previously sieved, so particle diameters in these preliminary experiments actually varied between approximately 150 and 500 μm.

Effect of particle diameter on random motility in porous media. To study the impact of particle diameter on the effective transport coefficients, silica sand was sieved as described previously to obtain samples relatively homogeneous in particle size. The sizes used ranged from 80 to 800 μm. Columns were constructed as described previously with sand of known particle size and distribution. Bacteria were initially localized in the bottom half of the columns and allowed to diffuse upward into the top half of the column, which initially contained only silica sand saturated with sterile mineral medium. The results are shown in Fig. 5 and 6. A general trend which indicates that the effective random motility of a bacterial population decreases with decreasing particle diameter is noted. In Fig. 5, curves generated by the model equations are superimposed on bacterial density profiles. Model curves simulate experimental results by averaging concentrations over sections of the continuous solution, analogous to a sectioned column.

Chemotaxis in porous media. In column experiments investigating chemotaxis, no measurable effect on penetration was observed. Experiments were conducted for several particle diameters (163, 194, and 274 μm) and attractant concentrations (5 and 20 mM). The attractant used was 3CB, which acts as a chemoattractant but cannot be degraded. In Fig. 7, results for

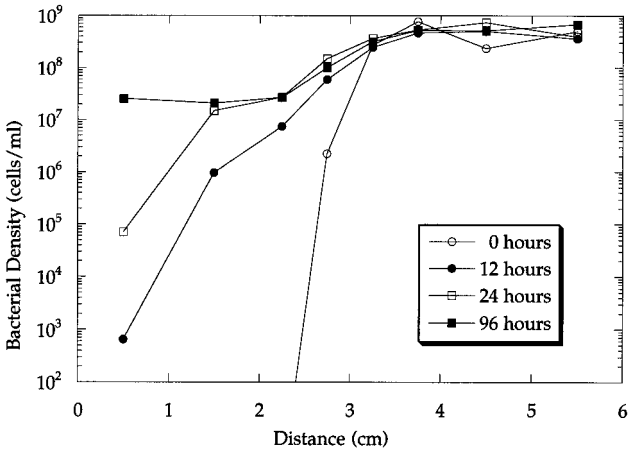

FIG. 4. Random motility of bacteria within a sand column. The bacterial density profiles above were obtained for the incubation times indicated in the figure. Initially, the lower half of the column (3 to 6 cm) was saturated with bacterial suspension while the top (0 to 3 cm) was saturated with sterile mineral medium. One column sectioned immediately (0 h) indicates the initial profile; in the upper half, only the section closest to and in contact with the interface contained detectable numbers of bacteria.

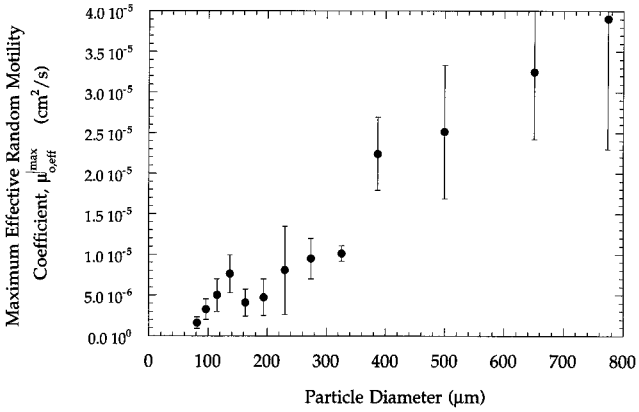

FIG. 6. Effective random motility coefficients decrease with decreasing particle diameter. Each point represents an average of 2 to 20 measurements. Sampling error increased as the average diameter used increased, presumably because of complications associated with sectioning columns filled with larger particles.

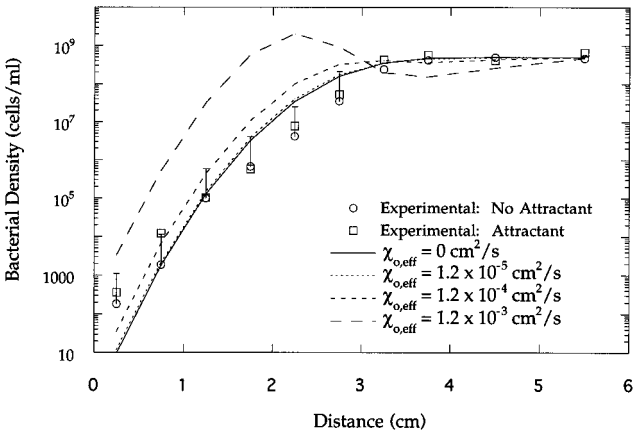

FIG. 7. Effect of chemotaxis on bacterial density profiles in sand columns. No significant differences between bacterial profiles obtained in the presence or absence of a 3CB gradient were noted. The model predictions presented above used $\mu_{0,eff}^{max} = 4.8 \times 10^{-6}$ cm^2/s. The average particle diameter was 194 μm. Experimental points are averages from two replicate columns. Error bars represent the standard deviation determined for the technique employed.

two typical columns, along with a model prediction, are displayed. The particle diameter used for this experiment was 194 μm, and the initial concentration of attractant (3CB) in the top half of the column was 5 mM. After 24 h, sections were analyzed and no statistically significant difference was evident with or without a 3CB gradient present. The associated numerical solutions assume that the chemotactic sensitivity coefficient is unaffected by the presence of the porous medium. When the coefficient is increased by an order of magnitude beyond its measured value, significant differences in model predictions are observed. Note, however, that this large value for the chemotactic sensitivity coefficient is not expected to fall within the physiologically relevant range for migration in porous media.

DISCUSSION

With growing interest surrounding in situ bioremediation as a treatment option for cleaning up contaminated soil, a few experimental studies (18, 22, 25, 26) have been aimed at determining rates of bacterial penetration through porous media. These studies have typically involved measurement of rates, in units of distance per time, which differ depending on the type of soil (physical characteristics and porosity) used. Penetration has typically been denoted by the time taken for at least one bacterium to reach the opposite end of saturated columns as determined by plate counts. Reynolds et al. (22) concluded that chemotaxis was unnecessary for penetration through a porous system and were unable to show penetration enhancement directly attributable to chemotaxis. López de Victoria (18) studied several subsurface isolates and their chemotactic response toward and/or away from trichloroethylene and noted rate enhancements from 10 μm/s to 20 μm/s for several strains when a trichloroethylene gradient was established within 30-cm columns filled with topsoil. Sharma et al. (26) improved upon this method of determining penetration rates of *E. coli* by sectioning columns at a given incubation time and determining bacterial density profiles throughout the column. This group concluded that a nonchemotactic *E. coli* mutant penetrated in a diffusive manner at a faster rate than its chemotactic parent. The chemotactic parent appeared to penetrate in an ordered or band-like fashion, suggesting that the mode of propagation may play a role in population migration. Studies by both Reynolds et al. (22) and Sharma and coworkers (25, 26) were conducted with anaerobic columns. Our column studies were conducted in an aerobic environment (which remained aerobic throughout the course of experiments, as verified by both oxygen microprobe [Microelectrodes, Inc.] and chemical indicator [resazurin]). As can be seen in Fig. 5, experimentally obtained curves indicated a diffusion-like process in the absence of a chemical gradient. This result was expected because the motile behavior of *P. putida* PRS2000 resembles a random walk in pure aqueous phase (12).

One significant trend discovered was that penetration declined with the average particle size utilized (Fig. 5 and 6). This was expected on the basis of analogies to Knudsen diffusion. The average cell swimming speed of *P. putida* PRS2000 in pure aqueous phase has been reported to be 44 μm/s (12). Cells typically swim from 1 to 3 s before momentarily stopping and changing direction. A mean run length would thus fall in the range of 50 to 150 μm. We hypothesize that as the interstitial spacing between particles declines, bacteria are increasingly unable to swim in a straight line for the normal duration of a run. For the smaller particle ranges used in these experiments (~100-μm diameters), this would be particularly true, and the matrix can be described as being very tortuous in terms of bacterial penetration. A similar result has been reported recently for motile *E. coli* strains in columns packed with glass beads; Sharma and McInerney (25) found that bacterial penetration rates increased linearly with bead size for chambers packed with 116-, 192-, and 281-μm-diameter beads. Rates were independent of bead size in chambers packed with larger 398- or 797-μm-diameter beads.

In order to predict bacterial migration due to motility in a subsurface environment, a mathematical relationship based on fundamental properties of the bacteria and the porous media is needed. Drawing on analogies to gaseous diffusion in a porous solid in which the effective diffusion coefficient is related to the molecular diffusion coefficient and properties of the porous media (24), an expression for the random motility coefficient of bacteria in porous media, μ_{eff}, is given by

$$\mu_{eff} = \frac{\varepsilon}{\tau}\mu \tag{7}$$

in which ε is porosity, τ is tortuosity, and μ is the random motility coefficient in the bulk aqueous phase. Given that no attractant gradients were present in the random motility experiments and assuming again that the decay rate in porous media was the same as in the bulk phase, μ_{eff} and μ in equation 7 can be replaced by $\mu_{0,eff}^{max}$ and μ_0^{max}, respectively. We determined the random motility coefficient for bacteria in the bulk phase and the porosity of the medium in independent experiments. The remaining parameter, tortuosity, accounts for the geometric effects of the porous media on the bacterial trajectories. However, tortuosity is not well defined in terms of easily measured properties of the porous matrix. Thus, it would be desirable to present the tortuosity of a porous medium in terms of pore diameter and other better-defined properties of the porous matrix. Duffy et al. (4) presented a theoretical expression for the tortuosity based on analogies to Knudsen diffusion, which suggested that the tortuosity increased in proportion to particle diameter, d_p^{-1}, for cases in which the average pore diameter, σ_p, was smaller than the mean bacterial run length. When the pore diameter is much larger than the run length of the bacteria, the motility is unaffected by the presence of the porous media (except for the excluded volume, which is accounted for by the porosity). Our experimental results were

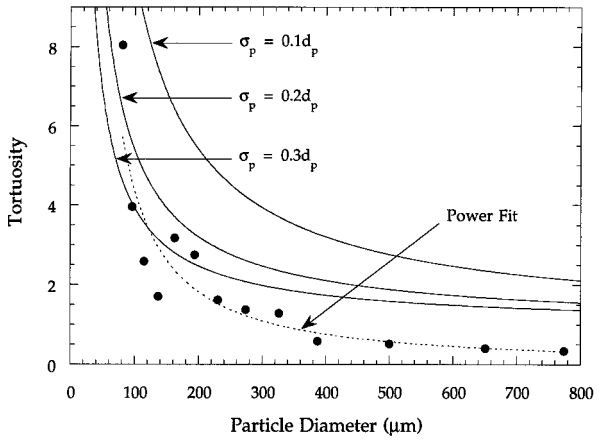

FIG. 8. Dependence of tortuosity on particle diameter. Tortuosity was found to be approximately inversely proportional to particle diameter. Equation 7 with $\varepsilon = 0.37$ and $\mu_0^{max} = 3.5 \times 10^{-5}$ cm^2/s was used to calculate values of tortuosity from experimental measurements of $\mu_{0,eff}^{max}$. A power fit of data yielded a dependence of $d_p^{-1.26}$, where d_p is the particle diameter, with $R = 0.91$.

consistent with this theoretical expression. In Fig. 8, tortuosities determined from experiments with bacteria migrating through saturated silica sand were plotted to show their dependence on particle diameter. Values of tortuosity varied between 0.5 and 8, decreasing with increasing particle size. Tortuosities were found to be inversely proportional to particle diameter. A power law fit of the data yielded an exponent of −1.26. Also plotted in Fig. 8 are three predictions of tortuosity based on the theoretical expression from Duffy et al. (4) for three values of f (0.10, 0.20, and 0.30). The parameter f is the ratio of pore diameter to particle diameter, which we used to estimate pore diameters. Qualitatively, the curves are similar to trends noted in the experimental data. Quantitative differences are believed to arise because of the value of k_{decay} (0.14 h^{-1}) used for determining $\mu_{0,eff}$. If this parameter was overestimated, then values for the tortuosity would be overestimated as well.

We conducted column experiments to investigate the effect of chemotaxis on penetration of *P. putida* through silica sand. As bacteria sense gradients established within porous media, we might expect them to respond by directing their migration in a nonrandom process toward increasing concentrations of chemoattractant. From our results, which included a number of geometries and attractant concentrations, we were not able to measure a statistically significant difference between migration rates in the presence or absence of a chemical gradient. In some experiments, bacterial density profiles obtained in the presence of an attractant gradient indicated a slightly higher penetration rate; in others, the reverse was noted. These differences were small however, and are within the range of the expected experimental error. In the aqueous phase, the chemotactic sensitivity coefficient was determined to be 1.9×10^{-4} cm^2/s. Model predictions made with similar values suggested that any enhancements would be small and difficult to distinguish given the limits in the sensitivity of our assay. Further complications may arise because of the presence of porous media and the nature of the chemotactic mechanism. Flagellar bacteria bias their migration toward increasing concentrations of attractant by altering their mean run length while swimming in a favorable direction. In other words, a pseudomonad might swim for 4 or 5 s before stopping and changing direction, rather than for 1 or 2 s. In these cases, the system effectively becomes more tortuous and encounters with sand particle surfaces become more likely. In a sense, the mechanism may be short-circuited by the medium matrix. Currently, no microscopic verification for this hypothesis exists.

Further investigations will delve into the effects of growth in saturated silica sand columns, including subsequent oxygen gradients which are expected to develop as degradation proceeds.

ACKNOWLEDGMENTS

This research was performed under appointment by J.W.B. to the Environmental Restoration and Waste Management Fellowship program administered by the Oak Ridge Institute for Science and Education for the U.S. Department of Energy. Part of the research (R.M.F.) was performed under the sponsorship of the U.S. Department of Energy Environmental Restoration and Waste Management Junior Faculty Award Program by the Oak Ridge Institute for Science and Education. The U.S. Environmental Protection Agency, Office of Exploratory Research (R819017-01-0), is also acknowledged for partial support of this research.

REFERENCES

1. **Bennett, C. O., and J. E. Myers.** 1982. Momentum, heat, and mass transfer, p. 500–501. McGraw-Hill, New York.
2. **Bird, R. B., W. E. Stewart, and E. N. Lightfoot.** 1960. Transport phenomena, p. 502. John Wiley & Sons, Inc., New York.
3. **Cohen-Bazire, G., W. R. Sistrom, and R. Y. Stanier.** 1957. Kinetic studies of pigment synthesis by non-sulfur purple bacteria. J. Cell. Comp. Physiol. **49:**25–68.
4. **Duffy, K. J., P. T. Cummings, and R. M. Ford.** 1995. Random walk calculations for bacterial migration in porous media. Biophys. J. **68:**800–806.
5. **Ford, R. M., and P. T. Cummings.** 1992. On the relationship between cell balance equations for chemotactic cell populations. SIAM J. Appl. Math. **52:**1426–1441.
6. **Ford, R. M., and D. A. Lauffenburger.** 1991. Measurement of bacterial random motility coefficients. II. Application of single-cell-based mathematical model. Biotechnol. Bioeng. **37:**661–672.
7. **Ford, R. M., B. R. Phillips, J. A. Quinn, and D. A. Lauffenburger.** 1991. Measurement of bacterial random motility and chemotaxis coefficients. I. Stopped-flow diffusion chamber assay. Biotechnol. Bioeng. **37:**647–660.
8. **Frymier, P. D., R. M. Ford, and P. T. Cummings.** 1993. Cellular dynamics simulations of bacterial chemotaxis. Chem. Eng. Sci. **48:**687–699.
9. **Frymier, P. D., R. M. Ford, and P. T. Cummings.** 1994. Analysis of bacterial migration. I. Numerical solution of balance equation. AICHE J. **40:**704–715.
10. **Gibson, D. T. (University of Iowa).** 1990. Personal communication.
11. **Harwood, C. S.** 1989. A methyl-accepting protein is involved in benzoate taxis in *Pseudomonas putida*. J. Bacteriol. **171:**4603–4608.
12. **Harwood, C. S., K. Fosnaugh, and M. Dispensa.** 1989. Flagellation of *Pseudomonas putida* and analysis of its motile behavior. J. Bacteriol. **171:** 4063–4066.
13. **Harwood, C. S., N. N. Nichols, M.-K. Kim, J. L. Ditty, and R. E. Parales.** 1994. Identification of the *pcaRKF* gene cluster from *Pseudomonas putida*: involvement in chemotaxis, biodegradation, and transport of 4-hydroxybenzoate. J. Bacteriol. **176:**6479–6488.
14. **Harwood, C. S., R. E. Parales, and M. Dispensa.** 1990. Chemotaxis of *Pseudomonas putida* toward chlorinated benzoates. Appl. Environ. Microbiol. **56:**1501–1503.
15. **Harwood, C. S., M. Rivelli, and L. N. Ornston.** 1984. Aromatic acids are chemoattractants for *Pseudomonas putida*. J. Bacteriol. **160:**622–628.
16. **Keller, E., and L. Segel.** 1971. Model for chemotaxis. J. Theor. Biol. **30:**225–234.
17. **Koshland, D. E., Jr.** 1980. Bacterial chemotaxis as a model behavioral system, p. 1–50. Raven Press, New York.
18. **López de Victoria, G.** 1989. M.S. thesis. University of Puerto Rico, Río Piedras Campus.
19. **Macnab, R. M.** 1987. Motility and chemotaxis, p. 732–759. *In* F. C. Neidhardt, J. L. Ingraham, K. B. Low, B. Magasanik, M. Schaechter, and H. E. Umbarger (ed.), *Escherichia coli* and *Salmonella typhimurium*: cellular and molecular biology, vol. 1. American Society for Microbiology, Washington, D.C.
20. **Macnab, R. M., and S.-I. Aizawa.** 1984. Bacterial motility and the bacterial flagellar motor. Annu. Rev. Biophys. Bioeng. **13:**51–83.
21. **Ordal, G. W.** 1985. Bacterial chemotaxis: biochemistry of behavior in a single cell. Crit. Rev. Microbiol. **12:**95–130.
22. **Reynolds, P. J., P. Sharma, G. E. Jenneman, and M. J. McInerney.** 1989. Mechanisms of microbial movement in subsurface materials. Appl. Environ. Microbiol. **55:**2280–2286.
23. **Rivero, M. A., R. T. Tranquillo, H. Buettner, and D. A. Lauffenburger.** 1989.

Transport models for chemotactic cell populations based on individual cell behavior. Chem. Eng. Sci. **44:**2881–2897.
24. **Satterfield, C. N., and T. K. Sherwood.** 1963. The role of diffusion in catalysis, p. 15. Addison-Wesley Publishing Company, Inc., Reading, Mass.
25. **Sharma, P. K., and M. J. McInerney.** 1994. Effect of grain size on bacterial penetration, reproduction, and metabolic activity in porous glass bead chambers. Appl. Environ. Microbiol. **60:**1481–1486.
26. **Sharma, P. K., M. J. McInerney, and R. M. Knapp.** 1993. In situ growth and activity and modes of penetration of *Escherichia coli* in unconsolidated porous materials. Appl. Environ. Microbiol. **59:**3686–3694.
27. **van der Meer, J. R., W. Roelofsen, G. Schraa, and A. J. B. Zehnder.** 1987. Degradation of low concentrations of dichlorobenzenes and 1,2,4-trichlorobenzene by *Pseudomonas* sp. strain P51 in nonsterile soil columns. FEMS Microbiol. Ecol. **45:**333–341.